DALTON

(*R*)- and (*S*)-2-Diphenylphosphinoyl-2′-hydroxy-1,1′-binaphthalene: versatile chiral bidentate ligands

Ronald J. Cross, Louis J. Farrugia, Paul D. Newman, Robert D. Peacock and Diane Stirling

Department of Chemistry, University of Glasgow, Glasgow G128QQ, UK

The homochiral compounds (*R*)- and (*S*)-2-diphenylphosphinoyl-2′-hydroxy-1,1′-binaphthalene, (*R*)- and (*S*)-Hbinappo, react with $TiCl_4$ or $ZrCl_4$ to produce complexes of bidentate binappo$^-$, $[MCl_2(binappo)_2]$ (M = Ti^{IV} or Zr^{IV}). VCl_3, $FeCl_3$ and MoO_2Cl_2 also react with Hbinappo, but require the presence of a base to produce $[M(binappo)_3]$ (M = V^{III} or Fe^{III}) or $[MoO_2(binappo)_2]$. The complex $[MoO_2(acac)_2]$ (acac = acetylacetonate) reacts with Hbinappo to produce $[MoO_2(acac)(binappo)]$. The vanadium(III) tris(chelate) complexes are readily oxidised in air to $[VO(binappo)_2]$. All of these complexes have been characterised by microanalytical, infrared, and, where appropriate, NMR, electronic and CD spectroscopic techniques. (*S*)-Hbinappo, $[ZrCl_2\{(S)\text{-binappo}\}_2]$, $[V\{(S)\text{-binappo}\}_3]$ and $[VO\{(S)\text{-binappo}\}_2]$ have also been characterised by single-crystal X-ray techniques. In all of the complexes the ligands are co-ordinated through their phenolate and phosphinoyl oxygen atoms forming eight-membered chelate rings. The tris-chelate complexes form stereospecifically, (*S*)-binappo giving the Λ isomer exclusively, and the (*R*)-form producing Δ-$[M(binappo)_3]$. Although each of the $[M(binappo)_3]$ species are necessarily sterically crowded, little M–O bond elongation is observed in the single-crystal X-ray structure of $[V\{(S)binappo\}_3]$. Initial attempts at achieving asymmetric induction in Ti^{IV}- and VO^{IV}-based oxidations of prochiral sulfides in the presence of these ligands are also presented, but observed enantiomeric excesses are generally < 10%.

The pursuit of new catalytic systems for the production of chiral materials from achiral or prochiral substrates is currently a prolific area of research for both inorganic and organic chemists. The range of reactions studied is large and still expanding with new methods being developed continuously, as emphasised by the inception of a number of journals solely dedicated to the chemistry of such systems. For metal-catalysed reactions, certain structural motifs within the ligands have been identified as being conducive to efficient chiral induction; one such group is that containing the 1,1′-binaphthyl unit **I**.

The preparation of the ligand (*S*)-Hbinappo, (*S*)-**II**, was first reported by Morgans and co-workers,[1] who discovered that the palladium(II) catalysed coupling of the bis(trifluoromethanesulfonate) ester of binaphthol with $Ph_2P(O)H$ terminated after the addition of a single diphenylphosphinoyl group (the disubstituted product desired by these workers was not obtained). Later, Hayashi and co-workers[2] reported an improved synthesis *en route* to substituted chiral monophosphines. In both of these cases the desired materials were phosphines, and the ligand properties of the phosphinoyl units were not explored. Previous work in our laboratories has shown that chiral phosphinoyl-alkoxides can be good bidentate ligands for early transition metals.[3] Moreover, they have potential as chiral auxiliaries in titanium(IV) and molybdenum(VI) based asymmetric oxidations. We have prepared the ligands, (*R*)- and (*S*)-Hbinappo, by a modification of the literature route and present here aspects of their co-ordination chemistry with early transition metals, as well as preliminary results pertaining to their potential for asymmetric induction as alluded to above.

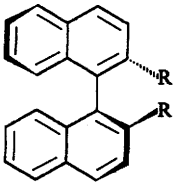

I

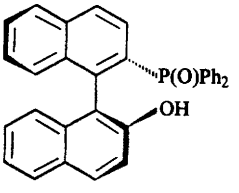

II

R = OH, NH_2,PPh_2 *etc.*

Results and Discussion

2-Diphenylphosphinyl-2′-hydroxy-1,1′-binaphthalene, Hbinappo II

(*R*)- and (*S*)-Hbinappo were prepared by the palladium catalysed phosphorylations of **I** (R = triflate) by a modification of a known procedure.[2] They were isolated as white solids, but recrystallisation from aqueous ethanol gave pale yellow crystals. Fig. 1 shows the X-ray crystal structure of (*S*)-Hbinappo, (*S*)-**II**, and salient bond lengths and bond angles are presented in Table 1. The torsion angle C(2)–C(1)–C(11)–C(16) between the two naphthyl rings systems is 76.6(4)°, and a strong internal hydrogen bond between the phosphoryl oxygen and the hydroxyl hydrogen is apparent [the O(1)···O(2) distance is 2.64(3) Å, with O(1)···H(2) 1.76(4) Å]. An aromatic stacking interaction between phenyl ring C(121)–C(126) of the diphenylphosphinoyl group and ring C(15)–C(20) of the naphthylol unit is apparent, with a plane separation of

Table 1 Important bond lengths (Å) and bond angles (°) for (*S*)-**II**

C(1)–C(2)	1.386(4)	C(1)–C(11)	1.504(4)
C(2)–P	1.816(3)	C(11)–C(12)	1.380(4)
C(12)–O(2)	1.372(4)	C(111)–P	1.800(3)
C(121)–P	1.739(3)	O(1)–P	1.495(2)
O(2)–H(2)	0.91(4)		
C(1)–C(2)–P	120.9(2)	C(3)–C(2)–P	118.9(2)
O(2)–C(12)–C(11)	122.0(3)	O(2)–C(12)–C(13)	117.2(3)
C(12)–O(2)–H(2)	105(3)	O(1)–P–C(121)	113.01(14)
O(1)–P–C(111)	109.84(13)	C(121)–P–C(111)	107.21(13)
O(1)–P–C(2)	111.73(12)	C(121)–P–C(2)	106.88(14)
C(111)–P–C(2)	107.92(13)		

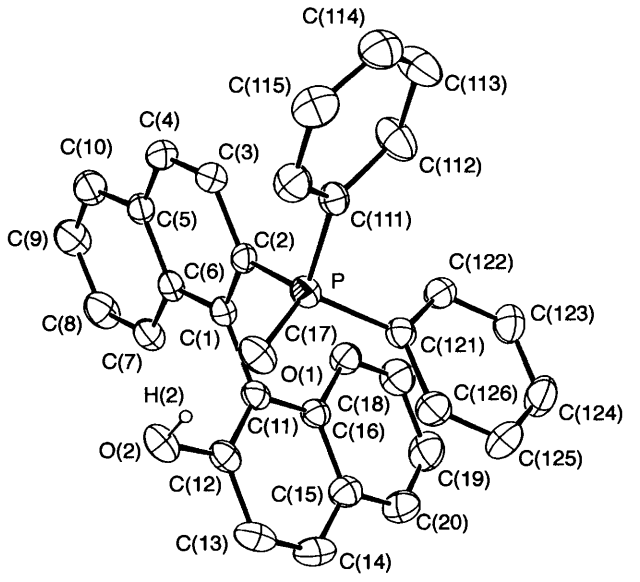

Fig. 1 The molecular structure and atomic labelling scheme of (*S*)-Hbinappo, (*S*)-**II** with thermal ellipsoids shown at the 30% probability level

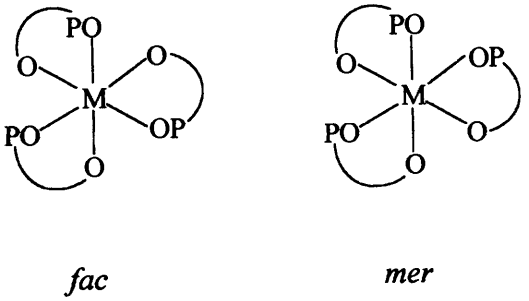

Fig. 2 *fac* and *mer* isomers of [M(binappo)$_3$]

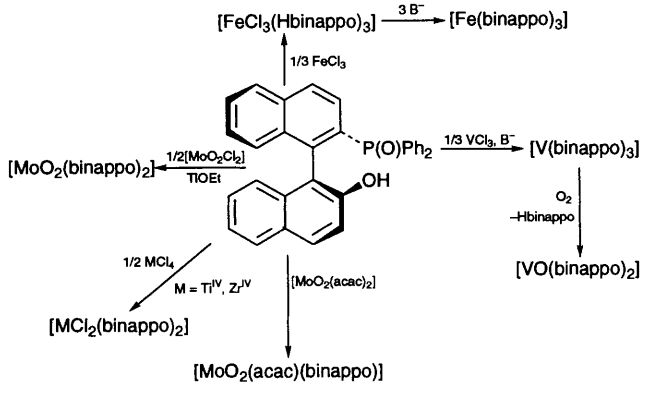

Scheme 1

approximately 3.6 Å. It is likely that this intramolecular interaction is responsible for the observed yellow colour *via* a bathochromic shift in the π–π^* transition induced by a charge-transfer interaction between these two aromatic systems. The P–O bond length of 1.495(2) Å is within the expected range for such units.

Complexes of (*R*)- and (*S*)-binappo

Two mole equivalents of (*S*)-Hbinappo reacted smoothly with $TiCl_4$ in tetrahydrafuran (thf) to give a deep red solution containing the [$TiCl_2$(binappo)$_2$] species after the loss of HCl. Removal of the solvent and recrystallisation from toluene–CH_2Cl_2 gave the titanium(IV) complex as an orange microcrystalline solid. Further recrystallisation from $CHCl_3$ gave deep red crystals which readily lost solvent molecules and so precluded X-ray analysis. The colourless [$ZrCl_2$(binappo)$_2$] analogue was prepared similarly, however, and recrystallisation from toluene–CH_2Cl_2 produced small, colourless crystals which were robust enough to allow single-crystal X-ray analysis. Both the titanium and zirconium complexes were stable to air and moisture.

Treatment of $FeCl_3$ or VCl_3 with three mole equivalents of the potassium salt of (*R*)- or (*S*)-binappo$^-$, prepared *in situ* by treating Hbinappo with KOBu^t, resulted in the isolation of the deep burgundy-red [Fe(binappo)$_3$] and golden-brown [V(binappo)$_3$] complexes, respectively. For these tris(chelate) complexes there are two possible geometric isomers, *facial* and *meridional* as depicted in Fig. 2. In addition, each geometric isomer may exist in two optical forms, *i.e.* Δ and Λ. As detailed below, for the [M(binappo)$_3$] complexes only *fac* isomers are formed, with absolute configurations about the metal determined by the chirality of the binaphthyl ligands; Λ for (*S*)-binappo, and Δ for (*R*)-binappo.

In the absence of a base, 3 mole equivalents of Hbinappo reacted with $FeCl_3$ in ethanol to give deep purple [$FeCl_3$(Hbinappo)$_3$] in which the neutral Hbinappo ligands appear to be co-ordinated through their phosphoryl oxygens only. The red, binary tris-chelate complexes could subsequently be obtained upon addition of 3 equivalents of base. It is likely that the [V(binappo)$_3$] complexes can also be prepared in these two stages, since reaction of VCl_3 with Hbinappo produces a colour change to green which is converted to orange [V(binappo)$_3$] on addition of base.

The crystals of [V(binappo)$_3$] proved air-sensitive, oxidising slowly, with the loss of one ligand to give the green vanadyl bis-(ligand) complexes. This oxidation was more rapid in solution and oxidation to [VO(binappo)$_2$] was complete in 12 h at room temperature. The vanadium(IV) complex was isolated as green crystals.

Stirring a solution of [MoO_2(acac)$_2$] with 1 mole equivalent of *S*-Hbinappo led to the elimination of Hacac and isolation of yellow [MoO_2(acac){(*S*)-binappo}]. IR bands at 936 and 907 cm^{-1} are indicative of a *cis*-MoO_2 arrangement. Treatment of a solution of [MoO_2Cl_2] with two mole equivalents of ligand gave yellow [MoO_2Cl_2{(*S*)-Hbinappo}$_2$], containing two monodentate neutral ligands. The ternary complex [MoO_2{(*S*)-binappo}$_2$] (also yellow) was subsequently obtained by treating [MoO_2Cl_2{(*S*)-Hbinappo}$_2$] with two mole equivalents of thallium(I) ethoxide. It, too, appears to contain a *cis*-MoO_2 unit (IR bands at 924 and 901 cm^{-1}).

The preparations of all of these complexes are summarised in Scheme 1.

Crystal structure determinations

Details of the data collections and subsequent structural solution for [V{(*S*)-binappo}$_3$], [VO{(*S*)-binappo}$_2$] and [$ZrCl_2$){(*S*)-binappo}$_2$] are given in the Experimental section.

[V{(*S*)-binappo}$_3$], **1** (Fig. 3), is a rare tris(oxygen chelate) complex of vanadium(III). Other examples are [V{Ph_2P(O)CH-$MeCO_2$}$_3$],[4] [V(acac)$_3$][5] and [V(cat)$_3$]$^{3-}$ (cat = catecholate).[6] It is the more remarkable in that it contains three eight-membered chelate rings, despite the considerable steric bulk of the binappo$^-$ ligands. Salient bond lengths and angles are presented in Table 2. The structure is slightly distorted away from octahedral, the main source of deviation being the disparate length of the V–O(C) and V–O(P) bonds (mean values 1.94 and 2.06 Å, respectively). The V–O(P) bonds are longer, and the V–O(C) bonds shorter, than those observed in the related tris[2-(diphenylphosphoryl)propanoato]vanadium(III) complex.[4] This probably reflects a stronger π-bonding contribution for phenolate *versus* a carboxylate oxygen. The V–O(phenolate)

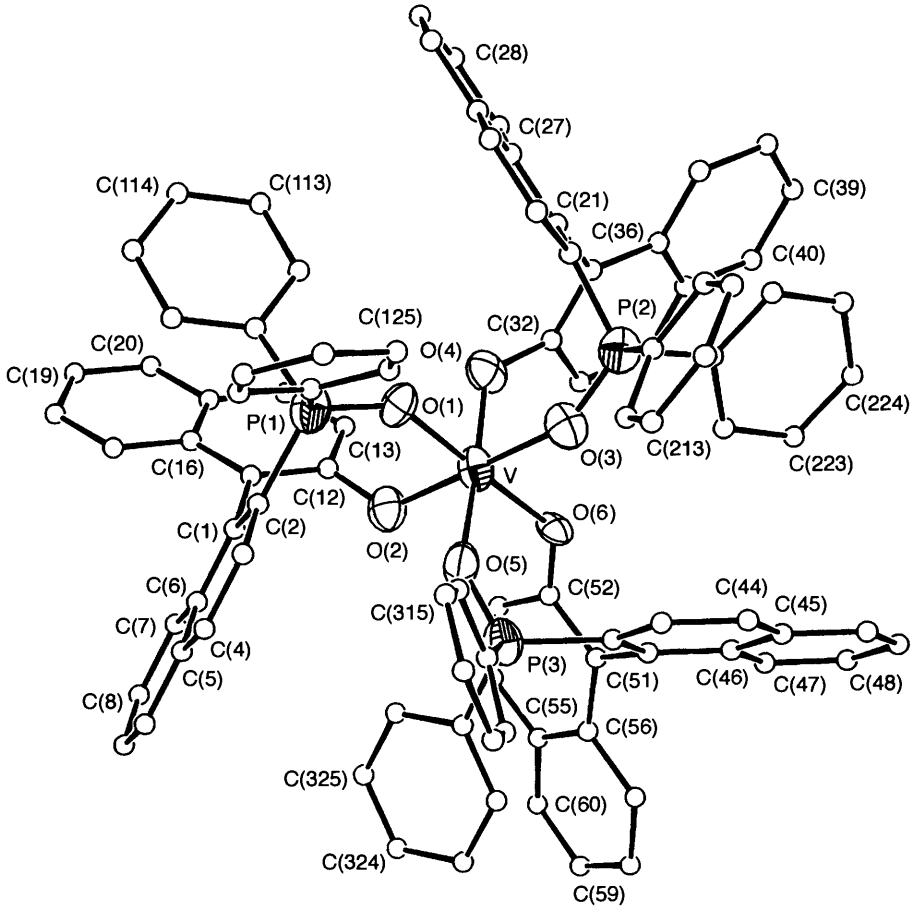

Fig. 3 The molecular structure and atomic labelling scheme of [V{(*S*)-binappo}$_3$] **1** with thermal ellipsoids shown at the 30% probability level; C atoms are shown as spheres of arbitrary radius

Table 2 Important bond lengths (Å) and angles (°) for molecule **1**

V–O(2)	1.922(11)	V–O(4)	1.952(11)
V–O(6)	1.938(10)	V–O(5)	2.033(12)
V–O(1)	2.058(10)	V–O(3)	2.075(11)
P(1)–O(1)	1.516(11)	P(1)–C(2)	1.800(9)
P(2)–O(3)	1.504(12)	P(2)–C(22)	1.807(9)
P(3)–O(5)	1.513(12)	P(3)–C(42)	1.821(8)
O(2)–C(12)	1.342(12)	O(4)–C(32)	1.380(12)
O(6)–C(52)	1.250(11)		
O(2)–V–O(4)	94.5(5)	O(2)–V–O(6)	96.3(6)
O(4)–V–O(6)	96.1(6)	O(2)–V–O(5)	87.9(5)
O(4)–V–O(5)	174.3(5)	O(6)–V–O(5)	88.8(4)
O(2)–V–O(1)	89.9(4)	O(4)–V–O(1)	87.0(5)
O(6)–V–O(1)	172.8(4)	O(5)–V–O(1)	87.8(4)
O(2)–V–O(3)	172.9(4)	O(4)–V–O(3)	89.6(4)
O(6)–V–O(3)	89.0(4)	O(5)–V–O(3)	87.5(4)
O(1)–V–O(3)	84.6(4)	O(1)–P(1)–C(2)	116.4(6)
O(3)–P(2)–C(22)	114.7(6)	O(5)–P(3)–C(42)	113.8(6)
P(1)–O(1)–V	139.3(7)	C(12)–O(2)–V	128.4(9)
P(2)–O(3)–V	141.7(7)	C(32)–O(4)–V	130.0(8)
P(3)–O(5)–V	141.3(6)	C(52)–O(6)–V	130.0(8)
O(2)–C(12)–C(11)	122.0(7)	O(2)–C(12)–C(13)	117.5(7)
O(4)–C(32)–C(33)	117.3(8)	O(4)–C(32)–C(31)	122.6(8)
O(6)–C(52)–C(51)	120.8(7)	O(6)–C(52)–C(53)	119.9(7)

bonds in [V(binappo)$_3$] are shorter than those observed in K_3[V(cat)$_3$]·1.5H_2O (2.013 Å),[6] but longer than those in [V(acacen)(thf)(OPh)] (1.881 Å) [H_2acacen = 4,4′-ethylenedinitrilobis(pentan-2-one)],[7] [V(salen)(py)$_2$][$ZnCl_3$(py)] (1.897 Å) [H_2salen = *N*,*N*′-bis(salicylidene)ethane-1,2-diamine][8] and [V(bbpen)]$^+$ (1.89 Å),[9] where bbpen^{2-} is the hexadentate bis(phenolate) of *N*,*N*′-bis(2-hydroxybenzyl)-*N*,*N*′-bis(2-methylpyridyl)ethane-1,2-diamine.

The phenolic O–V–O bond angles of 94.5–96.3° in [V(binappo)$_3$] are larger than the corresponding (P)O–V–O(P) angles, which are slightly compressed to 84.6–87.8°. Each set of three like donors (phosphoryl and phenolate) occupy a face of the octahedron defining the *facial* geometry. The absolute configuration is Λ, and the co-ordination of (*S*)-binappo to form [V(binappo)$_3$] is stereospecific. Likewise, circular dichroism (CD) spectra reveal the co-ordination of (*R*)-binappo to be similarly stereospecific giving the Δ isomer (see below). The conformations of the three eight-membered chelate rings are best described as boat-shaped. The torsion angles C(12)–C(11)–C(1)–C(2), C(32)–C(31)–C(21)–C(22) and C(52)–C(51)–C(41)–C(42) for the binaphthyl units at 72(1), 77(1) and 62(1)°, respectively, are quite similar to that of Hbinappo itself. It is remarkable that despite the obvious bulk of the three ligands there are no major distortions in the vanadium(III) co-ordination sphere.

Table 3 Important bond lengths (Å) and angles (°) for molecule **2**

V–O(3)	1.605(5)	V–O(2)	1.901(3)
V–O(1)	2.042(3)	P–O(1)	1.509(3)
P–C(12)	1.806(5)	O(2)–C(2)	1.342(5)
O(3)–V–O(2)	113.09(11)	O(2)–V–O(2′)	133.8(2)
O(3)–V–O(1)	101.75(10)	O(2)–V–O(1)	86.33(13)
O(2′)–V–O(1)	84.50(13)	O(1′)–V–O(1)	156.5(2)
O(1)–P–C(12)	113.9(2)	P–O(1)–V	140.3(2)
C(2)–O(2)–V	129.5(3)		

The structure of [VO{(*S*)-binappo}$_2$] **2** is shown in Fig. 4, with salient bond lengths and angles in Table 3. The co-ordination is distorted square pyramidal (see below), with an apical vanadyl oxygen and the four donors of the ligands forming the base. The ligands are bidentate, forming eight-membered chelates with bite angles of around 85°. Again, the

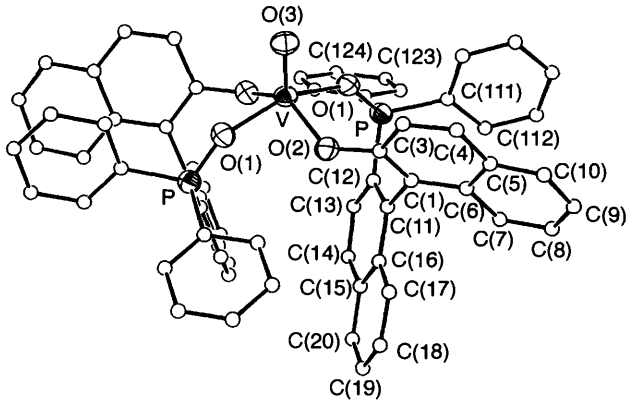

Fig. 4 The molecular structure and atomic labelling scheme of [VO{(*S*)-binappo}$_2$] **2** with thermal ellipsoids shown at the 30% probability level; C atoms are shown as spheres of arbitrary radius

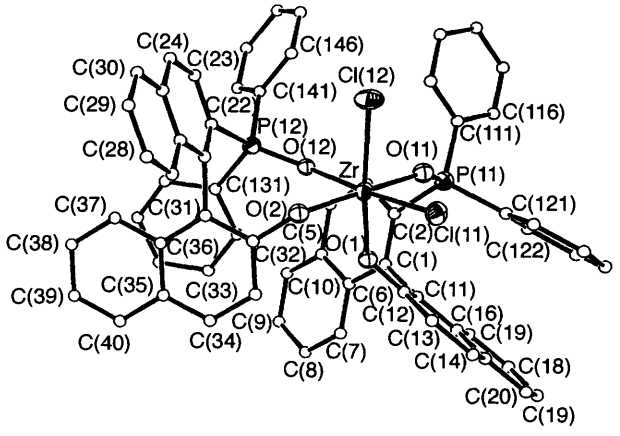

Fig. 5 The molecular structure and atomic labelling scheme of molecule **3a** of the complex [ZrCl$_2$\{(*S*)-binappo\}$_2$] with thermal ellipsoids shown at the 20% probability level; C atoms are shown as spheres of arbitrary radius

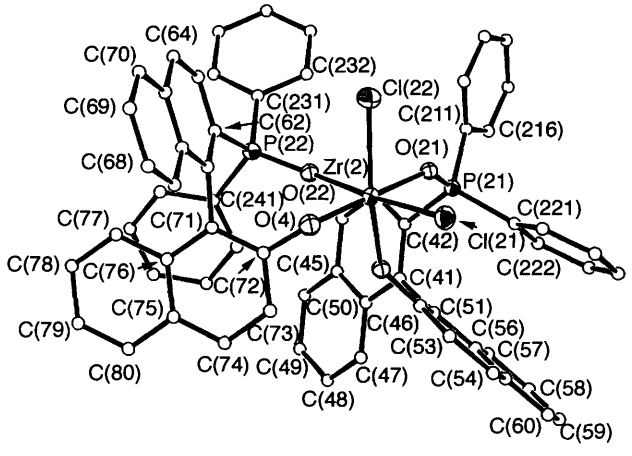

Fig. 6 The molecular structure and atomic labelling scheme of molecule **3b** of the complex [ZrCl$_2$\{(*S*)-binappo\}$_2$] with thermal ellipsoids shown at the 20% probability level; C atoms are shown as spheres of arbitrary radius

conformations of the chelate rings are best described as boat shaped, a geometry presumably demanded by the planarity and rigidity of the binaphthyl units. The phenolate donors (and, by necessity, the phosphoryl oxygens) are *trans*, and the two ligands are related by a crystallographic C_2 axis of rotation through the V=O bond. The V=O bond length is 1.605 Å, slightly longer than that in [VO(acac)$_2$],[10] but of similar length to that observed in [NH$_4$]$_4$[(VO)$_2$\{(+)-tart\}$_2$]·H$_2$O (H$_4$tart = tartaric acid).[11] The V–O(P) bond lengths in [VO(binappo)$_2$] (2.042 Å) are somewhat longer than those of the metal–phenolate distances (1.901 Å). As before, this disparity is not surprising; the V–O(phenolate) bonds are expected to contain appreciable d_π–p_π double-bond character as previously observed in similar systems.[12] It is noteworthy that the V–O(phenolate) bond lengths are shorter than those observed in K$_2$[VO(cat)$_2$]·EtOH·H$_2$O (1.956 Å),[13] [VO(L′)$_2$] (1.92 Å) (L′ = 2-methyl quinolin-8-olate),[14] and [VO(salpn)] (1.945 Å) [H$_2$salpn = *N*,*N*′-bis(salicylidene)propane-1,3-diamine)].[15]

There is an appreciable distortion away from an ideal square pyramid towards a trigonal-bipyramidal geometry in [VO(binappo)$_2$]. The O(P)–V–O(P) bond angle (156.5°) is more obtuse than that of (C)O–V–O(C) (133.8°), a situation akin to that found in the structure of [NH$_4$]$_4$[(VO)$_2$\{(+)-tart\}$_2$]·H$_2$O.[11] The vanadium atom is thus displaced by 0.75 Å from the (C)O···O(C) vector but only by 0.42 Å from the (P)O···O(P) vector. The binaphthyl units both have torsion angles similar to that observed in the uncomplexed (*S*)-Hbinappo [C(2)–C(1)–C(11)–(12) 74.9(7)°].

The unit cell of [ZrCl$_2$\{(*S*)-binappo\}$_2$] contains two independent molecules, **3a** and **3b**, shown in Figs. 5 and 6, respectively, with salient bond lengths and angles given in Table 4 for both. The co-ordination about the metal ion in both is distorted octahedral, and the two molecules differ only in minor respects, variations being mainly confined to differences in the torsional angles of the PPh$_2$ units. The arrangement of the donors about zirconium(IV) is all-*cis*, with absolute configuration Λ as defined by the two binappo$^-$ ligands. The torsion angle of the binaphthyl unit of one of the ligands is very similar to those found in the previous three structures [*e.g.* molecule **3a**, C(2)–C(1)–C(11)–C(12) 67(2)°] but the second such unit is twisted so that the naphthyl groups are nearer to orthogonal [*e.g.* molecule **3a**, C(22)–C(21)–C(31)–C(32) 99(2)°]. Such a twist is most likely a consequence of crystal-packing forces. The eight-membered chelate rings possess the same boat-like conformations observed in [V(binappo)$_3$] and [VO\{(*S*)-binappo\}$_2$]. The Zr–O(P) bond lengths average at 2.12 Å and are, as expected, longer than the Zr–O(C) vectors which average at 2.01 Å. The ligand bite angles are 80.6 and 84.8°, with the remaining octahedral angles being appropriately expanded or compressed. Previous workers have identified a number of structural features in metal–phenolate compounds as being sensitive to the extent of d_π–p_π character in the M–O bonds,[12] the lengths of M–O and C–O and the M–O–C angles being the most significant. In [ZrCl$_2$\{(*S*)-binappo\}$_2$], the Zr–O lengths are somewhat shorter than the expected value (2.07 Å),[16] and the Zr–O–C angle is expanded (140°). Although the latter may be restricted by the rigidity of the ligands, comparison with the vanadyl complex (V–O–C 130°) and the vanadium(III) complex (130°) suggest that the ligand is not entirely responsible, and that significant M–O(C) double bond character is evident in the zirconium(IV) complex. Further, the Zr–Cl bond *trans* to the phenolate donor is longer by *ca.* 0.04 Å with respect to that opposite the P=O donor. The probable intramolecular aromatic stacking feature observed in the structure of the free ligand is also evident in the crystal of [ZrCl$_2$\{(*S*)-binappo\}$_2$], which has aromatic ring separations of *ca.* 3.5 Å.

NMR spectra and solution structures

The ^{31}P and selected ^{13}C NMR data are presented in Table 5. The profusion of overlapping signals in the aromatic region of the ^{1}H NMR spectra renders this nucleus redundant for elucidation of intimate structural detail but the ^{31}P spectra are of value. For the [MCl$_2$(binappo)$_2$] complexes (M = Ti^{IV} or Zr^{IV}), there are five possible geometric isomers (Fig. 7). In the proton-decoupled ^{31}P spectrum of [ZrCl$_2$(binappo)$_2$], for which the solid-state structure has been determined, two equally intense signals are observed (Table 5). The crystal structure

Table 4 Important bond lengths (Å) and angles (°) for molecules **3a** and **3b**

3a		**3b**	
Zr(1)–O(2)	2.00(2)	Zr(2)–O(4)	1.95(2)
Zr(1)–O(1)	2.04(2)	Zr(2)–O(3)	2.02(2)
Zr(1)–O(11)	2.10(2)	Zr(2)–O(21)	2.15(2)
Zr(1)–O(12)	2.14(2)	Zr(2)–O(22)	2.18(3)
Zr(1)–Cl(11)	2.444(8)	Zr(2)–Cl(21)	2.44(2)
Zr(1)–Cl(12)	2.284(9)	Zr(2)–Cl(22)	2.50(2)
P(11)–O(11)	1.51(2)	P(21)–O(21)	1.57(2)
P(11)–C(2)	1.81(2)	P(21)–C(42)	1.793(13)
P(12)–O(12)	1.54(2)	P(22)–O(22)	1.50(2)
P(12)–C(22)	1.858(14)	P(22)–C(62)	1.825(12)
O(1)–C(12)	1.34(2)	O(3)–C(52)	1.356(10)
O(2)–C(32)	1.37(2)	O(4)–C(72)	1.332(11)
O(2)–Zr(1)–O(1)	93.3(7)	O(4)–Zr(2)–O(3)	91.9(7)
O(2)–Zr(1)–O(11)	169.6(7)	O(4)–Zr(2)–O(21)	172.4(7)
O(1)–Zr(1)–O(11)	80.6(7)	O(3)–Zr(2)–O(21)	83.2(7)
O(2)–Zr(1)–O(12)	84.8(6)	O(4)–Zr(2)–O(22)	85.9(7)
O(1)–Zr(1)–O(12)	89.6(7)	O(3)–Zr(2)–O(22)	90.5(6)
O(11)–Zr(1)–O(12)	86.7(6)	O(21)–Zr(2)–O(22)	88.3(7)
O(2)–Zr(1)–Cl(11)	97.6(5)	O(4)–Zr(2)–Cl(21)	95.1(5)
O(1)–Zr(1)–Cl(11)	94.5(5)	O(3)–Zr(2)–Cl(21)	93.5(5)
O(11)–Zr(1)–Cl(11)	91.3(5)	O(21)–Zr(2)–Cl(21)	91.0(5)
O(12)–Zr(1)–Cl(11)	175.1(5)	O(22)–Zr(2)–Cl(21)	175.8(5)
O(2)–Zr(1)–Cl(12)	98.8(6)	O(4)–Zr(2)–Cl(22)	100.5(6)
O(1)–Zr(1)–Cl(12)	166.3(5)	O(3)–Zr(2)–Cl(22)	166.8(5)
O(11)–Zr(1)–Cl(12)	86.4(6)	O(21)–Zr(2)–Cl(22)	84.0(5)
O(12)–Zr(1)–Cl(12)	85.0(5)	O(22)–Zr(2)–Cl(22)	85.9(6)
Cl(11)–Zr(1)–Cl(12)	90.4(3)	Cl(21)–Zr(2)–Cl(22)	89.9(3)
O(11)–P(11)–C(2)	109.6(9)	O(21)–P(21)–C(42)	111.6(5)
O(12)–P(12)–C(22)	114.7(9)	O(22)–P(22)–C(62)	114.4(4)
C(12)–O(1)–Zr(1)	141.0(13)	C(52)–O(3)–Zr(2)	142.9(6)
C(32)–O(2)–Zr(1)	132.1(13)	C(72)–O(4)–Zr(2)	134.7(7)
P(11)–O(11)–Zr(1)	148.1(12)	P(21)–O(21)–Zr(2)	139.5
P(12)–O(12)–Zr(1)	149.9(11)	P(22)–O(22)–Zr(2)	146.3

Table 5 Selected spectroscopic data for complexes of binappo$^-$ [a]

Complex	δ_P	δ_C	
		*C*O$^-$	*C*P(O)Ph$_2$
(*S*)-binappo	30.9	153.6	141.5
[MoO_2{(*S*)-binappo}$_2$]	32.7	165.4	144.0
[MoO_2(acac){(*S*)-binappo}]	34.7	163.0	*b*
[$ZrCl_2${(*S*)-binappo}$_2$]	41.2	161.5	*b*
	37.8	159.8	*b*
[$TiCl_2${(*S*)-binappo}$_2$]	42.1	166.6	143.5
	37.9	166.1	141.9
	41.3[c]		

[a] Recorded in $CDCl_3$ with reference to $SiMe_4$ (δ = 0 ppm) for ^{13}C or 85% H_3PO_4 (δ = 0 ppm) for ^{31}P. [b] Not assigned. [c] Minor isomer.

reveals the all-*cis* arrangement of donors, and if such a structure were maintained in solution, two equally intense ^{31}P peaks would be expected for each of the two unique P=O groups. As this appears to be the case, we propose that the solid-state structure is maintained in solution. We tentatively assign the low-field resonance to the P=O group *trans* to the phenolic oxygen, as we have previously observed that phosphoryl groups *trans* to alcoholate donors in titanium(IV) complexes resonate 10–12 ppm downfield to that of the uncomplexed ligand.[3]

The same ^{31}P NMR pattern is observed for [$TiCl_2$(binappo)$_2$], although a smaller peak indicative of a minor secondary isomer is observed. The presence of the single ^{31}P resonance for this minor isomer indicates the presence of a symmetry-related pair of P=O functions, and the relative chemical shift is at a position expected for a *trans* phenolic P=O function. The most likely structure, therefore, would appear to be the *trans-cis-cis* isomer, **4**.

The ^{31}P NMR spectrum of [MoO_2(acac){(*S*)-binappo}] contains a major signal at δ 34.7 and two minor ones at δ 40.2

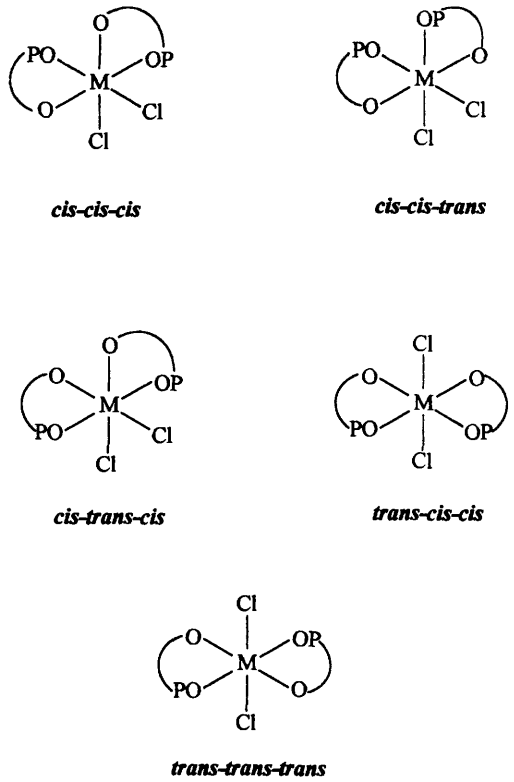

Fig. 7 Possible geometric isomers of [MCl_2(binappo)$_2$]

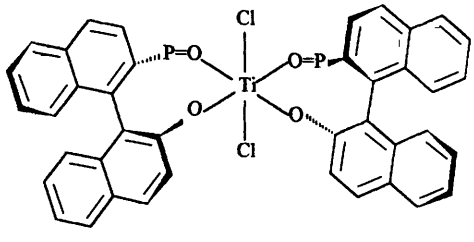

4

and 32.7. The resonance at δ 32.7 is assigned to a small amount of [MoO_2L_2] (see above) formed by the disproportionation reaction [equation (1)]. A comparable amount of

$$2[MoO_2(acac)(binappo)] \rightleftharpoons [MoO_2(binappo)_2] + [MoO_2(acac)_2] \quad (1)$$

[MoO_2(acac)$_2$] can be detected in the ^1H NMR spectrum of this system. The major and low-field minor signals are assigned to the two possible geometric isomers of [MoO_2(acac){(*S*)-binappo}] (assuming that the *cis*-MoO_2 unit is retained in solution), and we tentatively assign the major resonance to structure **5** on consideration of π-donor acidity–basicity complements of the *trans* donors; the relatively strongly d_π–p_π bonding phenolate oxygens would be reluctant to co-ordinate *trans* to the strong π-accepting/donating oxo groups.

That there is no rapid interconversion between these two isomers at room temperature is confirmed by the observation of two distinct methyl resonances for each isomer in the ^1H and ^{13}C NMR spectra. If the isomers were freely interconverting, the methyls would be observed as time-averaged single peaks.

The ^{31}P NMR spectrum of pure [MoO_2(*S*)-binappo}$_2$] shows a single resonance at δ 32.7 indicating either the formation of a single complex in solution with symmetry-related phosphoryl groups, or a mixture of rapidly interconverting isomers. The relative non-fluxionality of the

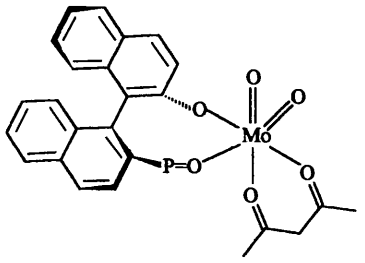

5

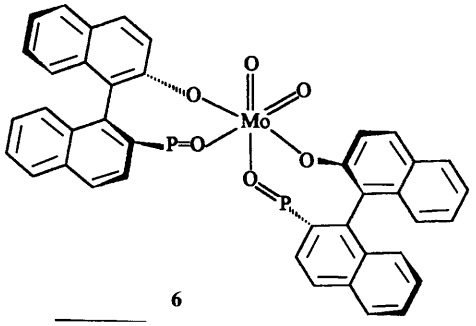

6

Table 6 Electronic and CD spectral details for complexes of binappo⁻ *

Complex	λ/nm (ε/dm³ mol⁻¹ cm⁻¹)	λ/nm (Δε/dm³ mol⁻¹ cm⁻¹)	$10^3\Delta\varepsilon/\varepsilon$
Λ-[Fe{(*S*)-binappo}$_3$]	499 (5 082)	483 (−5.37)	1.06
	332 (20 977)	412 (−13.18)	2.10
	318 (21 008)		
Δ-[Fe{(*R*)-binappo}$_3$]	503 (5 185)	500 (5.49)	1.06
	357 (21 691)	408 (13.18)	2.20
	332 (21 513)		
	320 (21 176)		
Λ-[V{(*S*)-binappo}$_3$]	729 (165)	720 (3.30)	20.0
	460sh (770)	480 (4.40)	5.70
		393 (−9.12)	2.05
Δ-[V{(*R*)-binappo}$_3$]	725 (169)	716 (−3.41)	20.2
	465sh (750)	483 (−4.38)	5.84
		390 (9.34)	2.13
(−)-[VO{(*S*)-binappo}$_2$]	885 (141)		
	703 (214)		
	620 (256)	625 (−1.59)	6.21
(+)-[VO{(*R*)-binappo}$_2$]	894 (113)		
	701 (181)		
	622 (216)	625 (1.61)	7.45

* Recorded in CH_2Cl_2.

[MoO_2(acac){(*S*)-binappo}] system supports the presence of a single isomer for [MoO_2{(*S*)-binappo}$_2$]. The small downfield shift of the ^{31}P resonance for [MoO_2{(*S*)-binappo}$_2$] with respect to (*S*)-Hbinappo would suggest little π bonding between the phosphinoyl oxygen and the metal. This is likely to be the case if the P=O function is co-ordinated opposite the strongly π-donating/accepting *cis*-oxo groups as observed in complexes of the type [$MoO_2X_2(OPPh_3)_2$],[17] and the most likely structure is the *cis-cis-trans* form, **6**.

Electronic and circular dichroism spectra

Relevant details are summarised in Table 6. The visible electronic spectra of the [V(binappo)$_3$] complexes consist of a long-wavelength component of relatively low intensity at ≈725 nm, and a shoulder to high energy of a charge-transfer (c.t.) band tailing from the UV, at around 465 nm. Two symmetrical CD maxima are observed with similar λ values to those described for the isotropic spectra. The sign of the CD bands are −,− for [V{(*R*)-binappo}$_3$] and +,+ for [V{(*S*)-binappo}$_3$]. These transitions have been assigned previously in like complexes as arising from the $^3T_{1g} \longrightarrow {}^3T_{2g}$ and $^3T_{1g} \longrightarrow {}^3T_{1g}(P)$ transitions of octahedral parentage.[18] However, these complexes approximate at best to D_3 symmetry, and the above-mentioned triplet states would be expected to be non-degenerate in such an environment. If so, the first transition would be split into $^3A_2 \longrightarrow {}^3E$ and $^3A_2 \longrightarrow {}^3A_1$ components. There is no evidence of this split in the CD spectrum, and it may be that the complex does approximate to O_h, or that one of the said components has a rotational strength sufficiently large to override the other. In the latter case, it is often implied from trigonal theory that the E component dominates the first absorption;[18] it has been shown that positive CD maxima are observed for Λ tris-chelates and negative for Δ.[18] It is known that [V{(*S*-binappo}$_3$] has the Λ configuration in the solid state, and indeed its spectrum has a positive long-wavelength component. By contrast, [V{(*R*-binappo}$_3$] shows enantiomeric CD, and is therefore assigned the Δ configuration.

Using the approximation to O_h symmetry, the CD maxima at 720 nm are assigned to the $^3T_{1g} \longrightarrow {}^3T_{2g}$ transition of O_h parentage, and the 480 nm transitions to the $^3T_{1g} \longrightarrow {}^3T_{1g}(P)$ promotion. These are both magnetic-dipole allowed in O_h symmetry, and this is consistent with the relatively large dissymmetry factors (Table 6). The third observable CD peak is lost in the tail of the intense charge-transfer absorptions in the isotropic spectrum. It may be assigned to the $^3T_{1g} \longrightarrow {}^3A_{2g}$ (O_h) transition, or to a c.t. component. The former is not allowed magnetically, and the latter is electric-dipole allowed; in each case, a small $\Delta\varepsilon/\varepsilon$ value would be expected, and this is seen to be the case. Using the position of the CD maxima for [V(binappo)$_3$], λ_{max} for the $^3T_{1g} \longrightarrow {}^3A_{2g}$ transition is calculated to be ≈275 nm. This is clearly not the case, and it seems likely that the high-energy CD maximum is c.t. in origin. The present complexes are rare examples of chiral tris(chelates) of V^{III}. The adoption of the Δ or Λ configuration is controlled by the chirality of the starting Hbinappo. Some examples of the resolution of vanadium(III) tris(chelates) are documented,[18] where the bidentate ligands are achiral, but these complexes racemise rapidly in solution. To our knowledge, this is the first example of the adoption and isolation of single configurational isomers of labile V^{III} containing three bidentate ligands, the stereochemistry being controlled by the co-ordination of the homochiral binappo ligands [it is known that tris(catecholate)-siderophore type ligands do form single configurational isomers with V^{III},[19] but these form a separate and unusual ligand series].

The stereoselective formation of Λ-[V{(*S*)-binappo}$_3$] and Δ-[V{(*R*)-binappo}$_3$] would be expected to be mimicked in the iron(III) complexes. The very closely similar infrared spectra of the vanadium(III) and iron(III) systems confirm the adoption of the *cis* geometry for the latter as determined crystallographically for Λ-*cis*-[V{(*S*)-binappo}$_3$]. The iron(III) complexes are high-spin d^5, and are therefore not expected to show any d–d features in the visible spectrum. The fact that they are highly coloured ($\varepsilon > 5000$ dm³ mol⁻¹ cm⁻¹) is associated with a charge-transfer absorption at ≈500 nm. The CD spectrum of Λ-*cis*-[Fe{(*S*)-binappo}$_3$] consists of two negative peaks; a broadened low-wavelength component and a symmetrical maximum at 412 nm. An enantiomorphic pattern is observed for Δ-*cis*-[Fe{(*R*)-binappo}$_3$] (Table 6). The low dissymmetry factors for these transitions confirm their electric-dipole allowed c.t. origin. Like V^{III}, high-spin iron(III) complexes are expected to be very labile. No Λ ⇌ Δ conversion is observed in solution for the optically pure complexes, and it is concluded that the chosen chirality of the binappo ligand controls the absolute stereochemistry of the resultant complexes. Interestingly, configurational isomers of [FeL_3] where L = achiral ligand have been resolved and shown by Abu-Dari and Raymond[20] to be relatively non-labile in solution.

Table 7 Catalytic oxidation of *p*-Tolylmethyl sulfide to *p*-tolylmethyl sulfoxide

Catalyst	Ti:L	Method[a]	Yield (%)	e.e.[b] (%) (confign.)
(*S*)-Hbinappo–Ti(OPr^i)$_4$	1:1	A	75	0
(*S*)-Hbinappo–Ti(OPr^i)$_4$	1:2	A	60	5 (*R*)
(*S*)-Hbinappo–Ti(OPr^i)$_4$	1:3	A	65	5 (*R*)
(*S*)-Hbinappo–Ti(OPr^i)$_4$	1:4	A	56	7 (*R*)
(*S*)-Hbinappo–Ti(OPr^i)$_4$	1:2	B	37	10 (*R*)
(*S*)-Hbinappo–Ti(OPr^i)$_4$	1:4	B	35	11 (*R*)
(*R*)-Hbinappo–Ti(OPr^i)$_4$	1:1	A	80	2 (*S*)
(*R*)-Hbinappo–Ti(OPr^i)$_4$	1:2	A	67	6 (*S*)
(*R*)-Hbinappo–Ti(OPr^i)$_4$	1:3	A	62	7 (*S*)
(*R*)-Hbinappo–Ti(OPr^i)$_4$	1:4	A	55	10 (*S*)
(*R*)-Hbinappo–Ti(OPr^i)$_4$	1:2	B	52	7 (*S*)
(*R*)-Hbinappo–Ti(OPr^i)$_4$	1:4	B	43	12 (*S*)
[VO{(*R*)-binappo}$_2$]		C	50	2 (*R*)
[VO{(*R*)-binappo}$_2$]		D	95	0

[a] Method A: sulfide–Ti(OPr^i)$_4$–Bu^{t}OOH = 1.0:0.1:1.0 in CCl_4 with activated sieves at −20 °C for 24 h. Method B: sulfide–Ti(OPr^i)$_4$–Bu^{t}OOH–H_2O = 1.0:0.1:1.0:0.1 in CCl_4 at 0 °C for 24 h. Method C: sulfide–[VO(binappo)$_2$]–Bu^{t}OOH = 1.0:0.1:1.0 at room temperature in CH_2Cl_2. Method D: sulfide–[VO(binappo)$_2$] = 1.0:0.1 with an excess of H_2O_2 in CH_2Cl_2 at room temperature. [b] e.e = Enantiomeric excess.

The isotropic spectra of the [VO(binappo)$_2$] complexes consist of 2 major, barely separated, maxima at ≈620 and 700 nm, and a relatively weak (broad) band at >880 nm. In C_{4v} symmetry, three d–d transitions are expected for five-co-ordinate VO^{2+}: (*i*) $^2B_2(d_{xy}) \longrightarrow {}^2E(d_{xz}, d_{yz})$; (*ii*) $^2B_2(d_{xy}) \longrightarrow {}^2B_1(d_{x^2-y^2})$; and (*iii*) $^2B_2(d_{xy}) \longrightarrow {}^2A_1(d_{z^2})$.[21] Band (*iii*) is often believed to be obscured by c.t. absorptions below 400 nm. The picture is further complicated by uncertainty in the relative ordering of the E and B_1 states, and, indeed, splitting of the E state in symmetries lower than C_{4v} {as is the case for [VO(binappo)$_2$]}. The CD spectra are of little assistance for band assignment in the present case. [VO{(*S*)-binappo}$_2$] gives a single negative maximum in the visible region, whereas [VO{(*R*)-binappo}$_2$] shows enantiomorphic behaviour with a single positive maximum (Table 6). The shape of the peaks are not entirely symmetrical, and it seems likely that the maxima at 620, 700 nm (isotropic) and the composite band at 625 nm (CD) represent the $^2B_2 \longrightarrow$ E transition of C_{4v} symmetry, albeit with loss of degeneracy in the upper state as a consequence of the true symmetry of the metal chromophore (C_2). Unfortunately, the isotropic maximum at λ > 880 nm was out of range of our CD instrumentation.

Catalysed chiral oxidation of sulfides to sulfoxides

Recent studies have shown that single enantiomers of binaphthol (**I**, R = OH) are effective auxiliaries for the titanium(IV)-catalysed oxidation of sulfides to sulfoxides.[22] Reactions were reported to proceed in two stages, with an enantioselective oxidation to sulfoxide being followed by a selective over-oxidation of the minor enantiomer to the sulfone, further enhancing the enantiomeric excess of the sulfoxide at the expense of yield. The presence of water enhanced both of these processes.

In view of the excellent ligand properties of our binappo$^-$ anion, we have tested (*R*)- and (*S*)-Hbinappo as chiral auxiliaries under similar conditions and on the same substrate in the expectation of improving the enantioselectivity of the binaphthol system. Results for the catalysed oxidation of *p*-tolylmethyl sulfide are summarised in Table 7. The observed enantiomeric excesses proved to be low, with a maximum of 12% [(*R*)] being seen for the reaction using a 4:1 ratio of (*R*)-Hbinappo to Ti(OPr^i)$_4$. The addition of 1 mole equivalent of water per titanium considerably slowed the reactions, and led to a small enhancement of the enantiomeric excess at the same time. The presence of the water presumably suppresses the operation of a more-rapid, non-selective pathway. Some over-oxidation to the sulfone (5–20%) was observed in most cases, but even if this had been selective to the major enantiomer produced (the opposite of the binaphthol case), the maximum obtainable enantiomeric excess from our systems would be low compared to the reported use of binaphthol. We conclude that Hbinappo may behave in a different way to binaphthol and that, although active, it does not make a useful chiral auxilliary in these catalytic systems.

Table 7 also lists the results of using [VO{(*R*)-binappo}$_2$] as catalyst for such oxidations. Although clearly behaving as an active catalyst, the enantiomeric excesses produced were negligible.

Experimental

NMR spectra were recorded on a Bruker AM 200 spectrometer operating in the Fourier transform mode. IR spectra were recorded on a Phillips PU 9800 spectrometer and UV/VIS spectra on a Perkin-Elmer Lambda 9. CD spectra were recorded on home-built apparatus. Microanalyses were carried out by Glasgow University Chemistry Department micro-analytical service.

(*S*)-2-Diphenylphosphinoyl-2′-hydroxy-1,1′-binaphthalene [(*S*)-Hbinappo]

This was prepared in accord with the literature method,[2] and obtained as a white solid after chromatography. Yield = 90% (Found: 81.3; H, 4.9. Calc. for $C_{32}H_{23}O_2P$: C, 81.70; H, 4.95%). IR(KBr): 3056m, 1962m, 1912w, 1892w, 1817w, 1769w, 1655w, 1618m, 1590m, 1570w, 1553m, 1512m, 1503m, 1483m, 1460m, 1451m, 1439vs, 1383m, 1370m, 1350m, 1312m, 1265w, 1258m, 1229s, 1186m, 1157vs, 1146s, 1138vs, 1119vs, 1092m, 1071m, 1026w, 1001w, 972w, 937w, 872m, 864m, 851w, 815vs, 774w, 750s, 741s, 725s, 706vs, 696vs, 687s, 669m, 633m, 625m, 583w, 567w, 540vs, 534s, 527vs, 457w, 453m and 432w cm^{-1}.

(*R*)-2-Diphenylphosphinoyl-2′-hydroxy-1,1′-binaphthalene [(*R*)-Hbinappo]

This was prepared in an analogous manner to the (*S*)-isomer (Found: C, 81.4; H, 4.9. Calc. for $C_{32}H_{23}O_2P$: C, 81.70; H, 4.95%). IR(KBr): 3056m, 1962m, 1912w, 1892w, 1817w, 1769w, 1655w, 1618m, 1590m, 1570w, 1553m, 1512m, 1503m, 1483m, 1460m, 1451m, 1439vs, 1383m, 1370m, 1350m, 1312m, 1265w, 1258m, 1229s, 1186m, 1157vs, 1146s, 1138vs, 1119vs, 1092m, 1071m, 1026w, 1001w, 972w, 937w, 872m, 864m, 851w, 815w, 774w, 750s, 741s, 725s, 706vs, 696vs, 687s, 669m, 633m, 625m, 583w, 567w, 540vs, 534s, 527vs, 457w, 453m and 432w cm^{-1}.

Dichlorobis[(*S*)-2-diphenylphosphinolyl-1,1′-binaphthalene-2′-olato]titanium(IV)

To a stirred solution of $TiCl_4$·2thf (100 mg, 0.3 mmol) in dichloromethane (25 cm^3) under nitrogen was added (*S*)-Hbinappo (2 mole equivalents) as a solid. An immediate colour change to deep red occurred on mixing. The solution was stirred for 2 h, pumped to dryness, stirred in hot MeCN (40 cm^3) for 10 min, and cooled to 30 °C. The resulting bright orange solid was isolated by filtration in air and recrystallised from toluene–CH_2Cl_2 at 4 °C. Yield = 200 mg (64%) (Found: C, 72.5; H, 4.2. Calc. for $C_{64}H_{44}Cl_2O_4P_2Ti$: C, 72.65; H, 4.20%). IR(KBr): 3054m, 1831w, 1781w, 1618m, 1590s, 1566w, 1551m, 1501m, 1458s, 1441s, 1424m, 1399w, 1368m, 1350s, 1321m, 1306m, 1271m, 1260m, 1223vs, 1159m, 1124vs, 1082vs, 1063vs, 1026m, 997w, 980vs, 939s, 874m, 851w, 820vs, 789w, 775m, 764vs, 745vs, 725vs, 702vs, 689s, 671s, 640vs, 627m, 617w, 596vs, 577s, 558vs, 542vs, 525vs, 519vs, 500s, 455w and 426w cm^{-1}.

Dichlorobis[(*S*)-2-diphenylphosphinoyl-1,1′-binaphthalene-2′-olato]zirconium(IV)–dichloromethane(4/1)

The colourless complex was prepared in an analogous manner to that described above for the titanium(IV) derivative, substituting $ZrCl_4$·2thf as the starting material. Yield = 240 mg (82%) (Found: C, 68.7; H, 4.2. Calc. for $C_{64.25}H_{44.5}Cl_{2.5}O_4P_2Zr$: C, 68.75; H, 4.00%). IR(KBr): 3056m, 1618m, 1591s, 1566m, 1554m, 1500m, 1485w, 1460vs, 1439s, 1426m, 1400w, 1372s, 1354s, 1327m, 1312m, 1275vs, 1260m, 1244vs, 1217w, 1194w, 1154m, 1125vs, 1080s, 1065vs, 1026m, 988s, 942m, 874w, 818s, 775w, 748s, 725m, 706s, 691s, 673m, 639s, 625w, 590m, 573m, 540vs, 519vs, 496m and 434w cm^{-1}.

Acetylacetonato[(*S*)-2-diphenylphosphinoyl-1,1′-binaphthalene-2′-olato]dioxomolydenum(VI)

To a stirred solution of $[MoO_2(acac)_2]$ (200 mg) in dichloromethane–toluene [25 cm^3 (1.5:1)] was added (*S*)-Hbinappo as a solid. The bright yellow solution was stirred for 1 h, concentrated *in vacuo* to 10 cm^3 and diluted with diethyl ether (10 cm^3). After storing overnight at 4 °C, the resulting bright yellow solid was filtered off, washed with diethyl ether and air-dried. Yield = 200 mg (47%) (Found: C, 63.3; H, 4.3. Calc. for $C_{37}H_{29}MoO_6P$: C, 63.80; H, 4.20%). IR(KBr): 3055m, 1962w, 1829w, 1725w, 1707w, 1601vs, 1590vs, 1557m, 1518vs, 1460s, 1439s, 1426s, 1373vs, 1352vs, 1331m, 1318m, 1271vs, 1260s, 1240vs, 1188m, 1157s, 1138s, 1117s, 1092m, 1067m, 1026m, 984s, 936vs, 907vs, 874m, 849w, 816s, 797w, 789w, 777m, 748s, 725s, 704vs, 693s, 673s, 654w, 639s, 625m, 617w, 590m, 573m, 554m, 538vs, 521vs, 471w, 444m and 407w cm^{-1}.

Λ-*cis*-Tris[(*S*)-2-diphenylphosphinoyl)-1,1′-binaphthalene-2′-olato]iron(III)

A solution of K[(*S*)-binappo] was prepared by the addition of potassium *tert*-butoxide (1 mole equivalent) to (*S*)-Hbinappo (170 mg) in ethanol (10 cm^3) under a nitrogen atmosphere. The solvent was removed under high vacuum, and the residue redissolved in ethanol (10 cm^3). This solution was then added dropwise *via* a cannula to a stirred solution of anhydrous $FeCl_3$ (20 mg) in ethanol (10 cm^3) under N_2. The pale yellow solution darkened during the addition, eventually becoming opaque, and subsequently precipitating a deep burgundy solid. The mixture was stirred for 1 h, then filtered in air, washed (ethanol then diethyl ether) and air-dried. The complex was desalted by dissolution in chloroform, filtering off KCl and removing the solvent to regain the burgundy coloured solid. Yield = 150 mg (83%) (Found: C, 79.2; H, 4.8. Calc. for $C_{96}H_{66}FeO_6P_3$: C, 78.75; H, 4.55%). IR(KBr): 3052m, 1962w, 1906w, 1821w, 1701w, 1686w, 1655w, 1614m, 1590s, 1555s, 1500s, 1485w, 1456vs, 1439s, 1424vs, 1400w, 1370vs, 1356vs, 1333m, 1312m, 1283vs, 1260s, 1248vs, 1213m, 1190m, 1156vs, 1148vs, 1138vs, 1115vs, 1094s, 1066m, 1026m, 988s, 872w, 849w, 818s, 795w, 775w, 743vs, 721s, 702vs, 673m, 639s, 625m, 588w, 569m, 538vs, 521vs, 492s, 430m and 411w cm^{-1}.

Λ-*cis*-Tris[(*S*)-2-diphenylphosphinoyl-1,1′-binaphthalene-2′-olato]vanadium(III)

To a stirred solution of VCl_3·3thf (73 mg) in thf under nitrogen was added, as a solid, (*S*)-Hbinappo (275 mg). The resultant green solution was stirred for 10 min before thallium(I) ethoxide (3 mole equivalents) was added. After stirring for 1 h, the mixture was filtered through Celite, and the orange filtrate pumped to dryness. The residue was crystallised from light petroleum (b.p. 40–60 °C)–CH_2Cl_2 by slow evaporation under N_2 to give golden-brown crystals. Yield = 150 mg (50%) (Found: 78.1; H, 4.7. Calc. for $C_{96}H_{66}O_6P_3V$: C, 79.00; H, 4.55%). IR(KBr): 3052m, 1964w, 1908w, 1821w, 1775w, 1736w, 1719w, 1701w, 1686w, 1676w, 1655w, 1638w, 1615m, 1590s, 1553m, 1501m, 1485m, 1453vs, 1439s, 1424s, 1368s, 1352vs, 1312m, 1275vs, 1258s, 1242vs, 1215s, 1192m, 1163s, 1148vs, 1138s, 1117s, 1094s, 1065m, 1026m, 997m, 984s, 939m, 872m, 849w, 820s, 814s, 795w, 741vs, 723s, 702vs, 673m, 639s, 627m, 588m, 569m, 540vs, 536vs, 525vs, 521vs, 484m, 451w and 432w cm^{-1}.

Bis[(*S*)-2-diphenylphosphinoyl-1,1′-binaphthalene-2′-olato]-oxovanadium(IV)

A solution of $[V\{(S)\text{-binappo}\}_3]$ (100 mg) in light petroleum–CH_2Cl_2 (15 cm^3, 1:2) was left to slowly air-oxidise at 4 °C over several days. The solution gradually became green, and subsequently green crystals precipitated. These were filtered off, washed very sparingly with cold CH_2Cl_2 to remove any free ligand and air-dried. Yield = 65 mg (95%) (Found: C, 76.4; H, 4.4. Calc. for $C_{64}H_{44}O_5P_2V$: C, 76.40; H, 4.40%). IR(KBr): 3056m, 1973w, 1831w, 1775w, 1736w, 1678w, 1655w, 1649w, 1638w, 1617w, 1592s, 1560w, 1501m, 1460vs, 1437m, 1424m, 1399w, 1372s, 1354s, 1331w, 1317w, 1279s, 1248s, 1217w, 1194w, 1165m, 1156m, 1136vs, 1117s, 1088m, 1067w, 1026w, 976vs, 941w, 874w, 822m, 816m, 750vs, 725s, 704vs, 694s, 681w, 673w, 639s, 625w, 594w, 573w, 563w, 559w, 538s, 525s, 449w and 428w cm^{-1}.

Bis[(*S*)-2-diphenylphosphinoyl-1,1′-binaphthalene-2′-olato]-dioxomolybdenum(VI)

(*S*)-Hbinappo (300 mg) was added as a solid to a stirred solution of $[MoO_2Cl_2]$ (64 mg) in thf (30 cm^3). To the yellow solution was added thallium(I) ethoxide (2 mole equivalents) and the mixture left to stir for 1 h; TlCl was filtered off through Celite, and the filtrate pumped to dryness. The yellow solid was stirred with diethyl ether for 15 min, filtered in air, washed (Et_2O) and air-dried. Yield = 200 mg (60%) (Found: C, 71.9; H, 4.3. Calc. for $C_{64}H_{44}MoO_6P$: C, 72.05; H, 4.15%). IR(KBr): 3054m, 1908w, 1823w, 1686w, 1655w, 1618m, 1589s, 1555m, 1501m, 1485w, 1460s, 1437s, 1426m, 1400w, 1372m, 1352s, 1318s, 1271s, 1260s, 1238vs, 1134vs, 1117vs, 1088s, 1067m, 1026w, 982s, 924s, 901vs, 874m, 849w, 816s, 799w, 777w, 747vs, 725s, 704vs, 694vs, 673m, 637s, 625m, 588w, 573w, 538vs, 523s, 488w, 432w and 411w cm^{-1}.

Trichlorotris[(*R*)-2-diphenylphosphinoyl-2′-hydroxy-1,1′-binaphthalene]iron(III)–water (1/1)

To a stirred solution of $FeCl_3$ (63 mg) in dry ethanol (10 cm^3) under N_2 was added (*R*)-Hbinappo (0.55 g) as a solid. The purple mixture was stirred for 1 h, then filtered in air to isolate the deep purple solid. A second crop of crystals was isolated on concentrating the filtrate. Yield = 350 mg (Found: C, 72.2; H, 4.6. Calc. for $C_{96}H_{71}Cl_3FeO_7P_3$: C, 72.40; H, 4.50%). IR(KBr): 3406br, 3056m, 2966w, 1973w, 1910w, 1831w, 1769w, 1686w, 1655w, 1617m, 1590m, 1561m, 1501m, 1460s, 1437s, 1426m, 1372m, 1352s, 1333w, 1318w, 1277s, 1264m, 1248vs, 1215w, 1192w, 1130vs, 1117s, 1082m, 1067m, 1049m, 1024w, 986m, 951w, 941w, 874w, 851w, 818m, 799w, 775w, 750s, 725m, 704vs, 694m, 679w, 673w, 637m, 625w, 590w, 571w, 554w, 536s, 525s, 430 and 403w cm^{-1}.

Δ-*cis*-Tris[(*R*)-2-diphenylphosphinoyl-2′-hydroxy-1,1′-binaphthalene]iron(III)

The complex was prepared as detailed for the analogous compound with (*S*)-binappo. Yield = 90% (Found: C, 78.0; H, 4.6. Calc. for $C_{96}H_{66}FeO_6P_3$: C, 78.75; H, 4.55%). IR(KBr): 3052m, 1962w, 1906w, 1821w, 1701w, 1686w, 1655w, 1614m, 1590s, 1555s, 1500s, 1485w, 1456vs, 1439s, 1424vs, 1400w, 1370vs, 1356vs, 1333m, 1312m, 1283vs, 1260s, 1248vs, 1213m, 1190m, 1156vs, 1148vs, 1138vs, 1115vs, 1094s, 1066m, 1026m,

Table 8 Experimental details of the crystallographic studies

Compound	(*S*)-**II**	**1**	**2**	**3**
Formula	$C_{32}H_{23}O_2P$	$C_{96}H_{66}O_6P_3V$	$C_{64}H_{44}O_5P_2V$	$C_{64}H_{44}Cl_2O_4P_2Zr$
M_r	470.47	1459.34	1005.87	1101.05
Space group	$P2_12_12_1$	$P4_1$	$P6_2$	$P2_1$
Crystal system	Orthorhombic	Tetragonal	Hexagonal	Monoclinic
a/Å	9.6121(9)	22.558(2)	22.182(7)	20.99(2)
b/Å	14.3240(9)	22.558(2)	22.182(7)	12.543(7)
c/Å	17.5028(12)	16.169(2)	10.610(2)	21.355(1)
β/°				90.99(5)
U/Å^3	2409.9(3)	8227.8(14)	4521(2)	5622(6)
θ range for cell/°	17.7–20.8	9.7–12.4	9.7–19.8	5.6–9.9
Z	4	4	3	4
D_c/g cm^{-3}	1.297	1.178	1.108	1.301
F(000)	984	3032	1563	2256
μ(Mo-Kα)/cm^{-1}	1.42	2.32	2.62	3.94
Scan mode	ω–2θ	ω–2θ	ω–2θ	ω–2θ
ω scan angle/°	0.54 + 0.45 tan θ	0.72 + 0.56 tan θ	0.52 + 0.48 tan θ	0.81 + 1.0 tan θ
θ range/°	2.3–25.0	2.4–19.5	2.2–25.0	2.5–20.5
Crystal size/mm	0.3 × 0.3 × 0.2	0.3 × 0.3 × 0.03	0.4 × 0.4 × 0.3	0.3 × 0.05 × 0.05
Absorption correction	None	None	Psi-scans	None
Max., min. transmission			0.94 to 0.89	
No. of data collected	3291	5688	4318	7607
No. of unique data	3052	4195	3118	6659
hkl Range	−1 to 11, −17 to 2, −2 to 20	−21 to 2, −2 to 21, −15 to 2	−23 to 2, −23 to 2, −1 to 12	−20 to 20, −1 to 12, −21 to 2
R_{int}	0.0198	0.0442	0.034	0.143
Standard reflections	(4 2 3) (−2 4 6) (−2 6 −4)	(−13 3 2) (−1 11 −1) (2 0 8)	(−6 8 3) (7 −3 4) (2 6 −3)	(0 5 −6) (−4 1 4) (4 2 4)
No. of data in refinement	3052	4195	3117	6659
No. of refined parameters	322	259	302	320
Final $R_1[I > 2\sigma(I)]$ (all data)	0.038 (0.058)	0.085 (0.143)	0.046 (0.067)	0.089 (0.187)
$wR_2[I > 2\sigma(I)]$ (all data)	0.086 (0.093)	0.212 (0.242)	0.120 (0.135)	0.214 (0.264)
Goodness of fit *S*	1.03	0.988	0.985	0.685
Absolute structure parameter	−0.27 (13)	0.36 (16)	−0.05 (5)	0.09 (14)
Largest remaining feature in electron density map/e Å^{-3}	0.17 (max.) −0.16 (min.)	0.48 (max.) −0.25 (min.)	0.32 (max.) −0.17 (min.)	0.45 (max.) −0.44 (min.)
Shift/e.s.d. in last cycle	0.007 (mean) −2.1 (max.)	0.0005 (mean) 0.001 (max.)	0.0005 (mean) 0.001 (max.)	0.0005 (mean) 0.001 (max.)

$R_1 = \Sigma(||F_o| - |F_c||)/\Sigma|F_o|$, $wR_2 = \{\Sigma[w(F_o^2 - F_c^2)^2]/\Sigma[w(F_o^2)^2]\}^{\frac{1}{2}}$, $R_{int} = \Sigma[F_o^2 - F_o^2(\text{mean})]/\Sigma F_o^2$, $S = \{\Sigma[w(F_o^2 - F_c^2)]/(n - p)\}^{\frac{1}{2}}$ where n = number of observations, p = number of refined parameters.

988s, 872w, 849w, 818s, 795w, 775w, 743vs, 721s, 702vs, 673m, 639s, 625m, 588w, 569m, 538vs, 521vs, 492s, 430m and 411w cm^{-1}.

Δ-*cis*-Tris[(*R*)-2-diphenylphosphinoyl-1,1′-binaphthalene-2′-olato]vanadium(III)

This was prepared as described for the corresponding complex containing (*S*)-binappo. Yield = 80% (Found: C, 78.1; H, 4.7. Calc. for $C_{96}H_{66}O_6P_3V$: C, 79.0; H, 4.55%). IR(KBr): 3052m, 1964w, 1908w, 1821w, 1775w, 1736w, 1719w, 1701w, 1686w, 1676w, 1655w, 1638w, 1615m, 1590s, 1553m, 1501m, 1485m, 1453vs, 1439s, 1424s, 1368s, 1352s, 1312m, 1275vs, 1258s, 1242vs, 1215s, 1192m, 1163s, 1148vs, 1138vs, 1117s, 1094s, 1065m, 1026m, 997m, 984s, 939m, 872m, 849w, 820s, 814s, 795w, 741vs, 723s, 702vs, 673m, 639s, 627m, 588w, 569m, 540vs, 536vs, 525vs, 521vs, 484m, 451w and 432w cm^{-1}.

Bis[(*R*)-2-diphenylphosphinoyl-1,1′-binaphthalene-2′-olato]-oxovanadium(IV)

This was synthesised in like fashion to the above complex of (*S*)-binappo, except that the solution was allowed to oxidise at room temperature. Yield = 75% (Found: C, 75.9; H, 4.6. Calc. for $C_{64}H_{44}O_5P_2V$: C, 76.40; H, 4.40%). IR(KBr): 3056m, 1973w, 1831w, 1775w, 1736w, 1678w, 1655w, 1649w, 1638w, 1617w, 1592s, 1560w, 1501m, 1460vs, 1437m, 1424m, 1399w, 1372s, 1354s, 1331w, 1317w, 1279s, 1248s, 1217w, 1194w, 1165m, 1156m, 1136vs, 1117s, 1088m, 1067w, 1026w, 976vs, 941w, 874w, 822m, 816m, 750vs, 725s, 704vs, 694s, 681w, 673w, 639s, 625w, 594w, 573w, 563w, 559w, 538s, 525s, 449w and 428w cm^{-1}.

Catalytic oxidations

Method A. To a stirred solution of $Ti(OPr^i)_4$ (90 mg) in dry CCl_4 (40 cm^3) at −20 °C under N_2 was added powdered activated molecular sieves and (*R*)- or (*S*)-Hbinappo (1–4 mole equivalents). After stirring for 30 min, *p*-tolylmethyl sulfide (440 mg, 10 mole equivalents) was added, followed, after a period of 20 min, by the addition of Bu^tOOH (5.5 mol dm^{-3} in nonane, 0.58 cm^3, 10 mole equivalents). The mixture was left at 20 °C overnight, then filtered, washed with Na_2SO_3(aq), dried with anhydrous $MgSO_4$ and concentrated *in vacuo* to a yellow-brown oil. This was analysed by ^{1}H NMR spectroscopy in the presence of the chiral shift reagent (*S*)-*N*-(3,5-dinitrobenzoyl)-2-methylbenzylamine to establish the enantiomeric excess of the resultant sulfoxide.

Method B. To a stirred solution of $Ti(OPr^i)_4$ (90 mg) in dry CCl_4 (40 cm^3) at −20 °C under N_2 was added (*R*)- or (*S*)-Hbinappo (2 or 4 mole equivalents). Water (6 mm^3, 1 mole equivalent) was added to the yellow-brown solution and stirring was maintained at room temperature for 1 h. *p*-Tolylmethyl sulfide (440 mg, 10 mole equivalents) was added and the mixture stirred for 20 min at 0 °C. A solution of Bu^tOOH (5.5 mol dm^{-3} in nonane, 0.58 cm^3, 10 mole equivalents) was next added and the mixture left overnight at 0 °C. The solution was then hydrolysed by addition of water (1 cm^3), filtered and the filtrate shaken with aqueous Na_2SO_3 and dried over anhydrous

$MgSO_4$. The resulting yellow oil was concentrated and analysed as above.

Method C. To a solution of [VO{(*R*)-binappo}$_2$] (12 mg, 1.2×10^{-5} mole) in dry CH_2Cl_2 (10 cm^3) at 0 °C under N_2 was added *p*-tolylmethyl sulfide (165 mg, 100 mole equivalents) then, after 20 min, Bu^{t}OOH (5.5 mol dm^{-3} in nonane, 0.22 cm^3, 100 mole equivalents). This mixture was left at 10 °C overnight then worked up as detailed above.

Method D. As for method C, but with 30 v/v H_2O_2 replacing the Bu^{t}OOH.

Experimental details of the structure determinations

General procedures. Details of data collection procedures and structure refinement are given in Table 8. Single crystals of suitable size were attached to a glass fibre using acrylic resin, and mounted on a goniometer head in a general position. Data were collected at ambient temperature on an Enraf-Nonius TurboCAD4 diffractometer, running under CAD4-Express software, and using graphite-monochromated Mo-Kα X-radiation (λ = 0.710 73 Å). Unit-cell dimensions were determined by refinement of the setting angles of 14–25 reflections which were flagged during data collection. Standard reflections were measured every 2 h during data collection, and an interpolated correction was applied to the reflection data where necessary. Lorentz-polarization corrections were also applied to the reflection data. $\sigma(F_o)^2$ was estimated from counting statistics. The structures were solved by direct methods (SIR 92),[23] and refined by full-matrix least-squares using SHELXL 93.[24] Aliphatic and aromatic CH hydrogen atoms were included at calculated positions, with C–H 0.96 Å. The naphthalene rings in all the structures of the metal complexes were refined as idealised groups using the AFIX 11 option in SHELXL 93.[24] Neutral-atom scattering factors and coefficients of anomalous dispersion were obtained from ref. 25. The known absolute (*S*) configuration of the binaphthol ring system was applied to each structure, although the refined value of the Flack absolute structure parameter[26] confirmed this configuration in all cases.

Specific details. (*S*)-**II**. Crystals grow as pale straw coloured prisms. No absorption correction was applied. All non-H atoms were allowed anisotropic thermal motion. Refinement used the weighting scheme $w = [\sigma^2(F_o)^2 + (0.0491P)^2 + 0.0429P]^{-1}$ where $P = [F_o^2/3 + 2F_c^2/3]$.

1. Crystals grow as pale-brown prisms. The crystal diffracted poorly, and slowly converted to compound **2**. It was hence decided to terminate data collection at $\theta \approx 20°$. No absorption correction was applied. In view of the paucity and low resolution of the data set, only the V, P and O atoms were allowed anisotropic thermal motion. Refinement used the weighting scheme $w = [\sigma^2(F_o)^2 + (0.1345P)^2 + 8.5273P]^{-1}$ where $P = [F_o^2/3 + 2F_c^2/3]$.

2. Crystals grow as deep green prisms. A semi-empirical absorption correction (ψ scans using nine reflections with $\chi \geqslant 70.6°$) was applied to the data set. All non-H atoms were allowed anisotropic thermal motion. Refinement used the weighting scheme $w = [\sigma^2(F_o) + (0.0858P)^2]^{-1}$ where $P = [F_o^2/3 + 2F_c^2/3]$.

3. ψ-Scans using nine reflections with $\chi \geqslant 80.7°$ were measured, but analysis revealed no systematic variation in intensities. An absorption correction was thus deemed unnecessary. The crystal diffracted poorly, and it was decided to terminate data collection at $\theta \approx 20°$. In view of the paucity and low resolution of the data set, only the Zr, P and Cl atoms were allowed anisotropic thermal motion. Calculations using PLATON[27] revealed a void at the centre of the unit cell, which was probably occupied by a severely disordered solvent molecule(s). The residual density peaks ($\approx$1 e $Å^{-3}$) were not sufficient to determine the nature of the included solvent, and the 'solvent' contributions were removed from the structure factors by the SQUEEZE procedure of van der Sluis and Spek.[28] Refinement used the weighting scheme $w = [\sigma^2(F_o)^2 + (0.1729P)^2]^{-1}$ where $P = [F_o^2/3 + 2F_c^2/3]$.

Atomic coordinates, bond lengths and angles, and thermal parameters have been deposited at the Cambridge Crystallographic Data Centre (CCDC). See Instructions for Authors, *J. Chem. Soc., Dalton Trans.*, 1996, Issue 1. Any request to the CCDC for this material should quote the full literature citation and the reference number 186/225.

Acknowledgements

We wish to thank C. Scott of this University for a gift of (*S,S*)- and (*R,R*)-binaphthol, and gratefully acknowledge the support of the EPSRC (Process Engineering Separations Initiative; grant number GR/J 45190).

References

1 L. Kurz, G. Lee, D. Morgans, jun., M. J. Waldyke and T. Ward, *Tetrahedron Lett.*, 1990, **31**, 6321.
2 Y. Uozumi, A. Tanahashi, S-Y. Lee and T. Hayashi, *J. Org. Chem.*, 1993, **58**, 1945.
3 R. J. Cross, L. J. Farrugia, P. D. Newman, R. D. Peacock and D. Stirling, *J. Chem. Soc., Dalton Trans.*, 1996, 1637.
4 R. J. Cross, L. J. Farrugia, P. D. Newman, R. D. Peacock and D. Stirling, *J. Chem. Soc., Dalton Trans.*, 1996, 1087.
5 B. Morosin and H. Montgomery, *Acta Crystallogr., Sect. B*, 1969, **25**, 1354.
6 S. R. Cooper, Y. B. Koh and K. N. Raymond, *J. Am. Chem. Soc.*, 1982, **104**, 5092.
7 M. Mazzanti, C. Floriani, A. Chiesi-Villa and C. Guastini, *Inorg. Chem.*, 1986, **25**, 4158.
8 M. Mazzanti, S. Gambarotta, C. Floriani, A. Chiesi-Villa and C. Guastini, *Inorg. Chem.*, 1986, **25**, 2308.
9 A. Neves, A. S. Ceccato, S. M. D. Erthal, I. Vencato, B. Nuber and J. Weiss, *Inorg. Chim. Acta*, 1991, **187**, 119.
10 P. K. Hon, R. L. Bedford and C. E. Pfluger, *J. Chem. Phys.*, 1965, **43**, 3111.
11 G. J. Forrest and C. K. Prout, *J. Chem. Soc. A*, 1967, 1312.
12 U. Auerbach, T. Weyhermeyer, K. Wieghardt, B. Nuber, E. Bill, C. Butzlaff and A. X. Trautwein, *Inorg. Chem.*, 1993, **32**, 508.
13 S. R. Cooper, Y. B. Koh and K. N. Raymond, *J. Am. Chem. Soc.*, 1982, **104**, 5092.
14 M. Shiro and Q. Fernando, *Chem. Commun.*, 1971, 63.
15 M. Matthew, A. J. Carthy and G. J. Palenik, *J. Am. Chem. Soc.*, 1970, **92**, 3197.
16 A. G. Orpen, L. Brammer, F. H. Allen, O. Kennard, D. G. Watson and R. Taylor, *International Tables for Crystallography*, ed. A. J. C. Wilson, Kluwer, Dordrecht, 1995, vol. C, section 9.6.
17 R. J. Butcher, B. R. Penfold and E. Sinn, *J. Chem. Soc., Dalton Trans.*, 1979, 668.
18 R. D. Gillard, D. J. Sheperd and D. A. Tarr, *J. Chem. Soc., Dalton Trans.*, 1976, 594.
19 A. R. Bulls, C. G. Pippin, F. E. Hahn and K. N. Raymond, *J. Am. Chem. Soc.*, 1990, **112**, 2627.
20 K. Abu-Dari and K. N. Raymond, *J. Am. Chem. Soc.*, 1977, **99**, 2003.
21 J. Selbin, *Coord. Chem. Rev.*, 1966, **1**, 293.
22 N. Komatsu, M. Hashizume, T. Sugita and S. Uemura, *J. Org. Chem.*, 1993, **58**, 4529.
23 SIR 92, a program for automatic solution of crystal structures by direct methods. A. Altomare, G. Cascarno, C. Giacovazzo and A. Gualiardi, *J. Appl. Crystallogr.*, 1994, **27**, 435.
24 SHELXL 93 a program for crystal structure refinement, G. M. Sheldrick, University of Göttingen, 1993.
25 *International Tables for Crystallography, Volume C Mathematical, Physical and Chemical Tables*, Kluwer, Dordrecht, 1995, Tables 4.2.4.2, 4.2.6.8 and 6.1.1.4.
26 H. D. Flack, *Acta Crystallogr., Sect. A*, 1983, **39**, 876.
27 PLATON, A. L. Spek, *Acta Crystallogr., Sect.A*, 1990, **46**, C34.
28 P. van der Sluis and A. L. Spek, *Acta Crystallogr., Sect.A*, 1990, **46**, 194.

Received 5th June 1996; *Paper* 6/03952I